Tilicho Lake Origin: Valley Damming by a Giant Rockslide

Shayan Khatiwada[1*], Jérôme Lavé[2], Marius Huber[2], Luc Scholtès[3] & Ananta Prasad Gajurel[4]

[1]*M.Sc. in Mountain and Mountaineering Sciences, Nepal Mountain Academy, Tribhuvan University, Kathmandu*
[2]*CRPG, CNRS, Université de Lorraine, Vandoeuvre les Nancy, France*
[3]*Laboratoire Magmas et Volcans, Clermont Ferrand, France*
[4]*Department of Geology, Tri-Chandra Multiple Campus, Tribhuvan University, Kathmandu*
[*]*Corresponding Author: jerome.lave@univ-lorraine.fr*
DOI: http://doi.org/10.3126/jtha.v8i1.96409

Abstract

The origin of the Tilicho Lake, located at 4,919 meters in Nepal's Manang district, has never been elucidated so far. In this study, based on observations along the Upper Marsyandi of a 12-km-wide deposit that exhibits typical rock avalanche facies, we propose that Tilicho lake was formed by a massive rockslide that blocked the Upper Marsyandi valley. The similar carbonate isotopic signature of the rockslide debris found in the upper Marsyandi and Phache valleys suggests the breccia deposit filled these two valleys and originated from Upper Ordovician to Middle Devonian strata. Lithologic and geomorphic arguments suggest that the rockslide resulted from the collapse of the Khansar Kan ridge, located South-East of the Tilicho lake. According to the estimated breccia deposit volume of 21 km^3 made previously by Huber (2024), we realized a reconstruction of the collapsed paleosummit and a numerical modeling of the rock avalanche dynamics. The paleosummit would have culminated at around 8400 meters, and the resulting rockslide deposit would have reached an extent of about 96 km^2. The modeled geometry of the rock avalanche is close to the observed one, confirming that the rockslide's damming created Tilicho Lake and smaller lakes in Phache valley. This catastrophic event has deeply reshaped the landscape of this region, highlighting the role of large-scale rockslides in landscape evolution in mountainous regions.

Keyword: landscape evolution, Manang, massive rockslide, rock avalanche modeling, Tilicho Lake

Introduction

Tilicho Lake is a lake located in the Manang district of Nepal (Figure 1a). It is situated at an altitude of 4,919 meter above sea level (masl), north of the Annapurna Range and south of the Chulu Himal. Tilicho Lake is considered as Nepal's highest large lake (surface area larger than 1 km^2), with a length of 4 km and a width of 1.2 km. Its maximum depth reaches 95 m with most of the lake being deeper than 60 m (Aizaki et al., 1987), and contains around 0.15 cubic kilometer of fresh glacial water, whose surface freezes in winter. Its watershed lies in the north of Tilicho mountain range and falls in the rain shadow area of the Annapurna Range. The lake is fed by perennial streams that are originating by snow and glacier melts.

Today, Tilicho Lake is the destination of one of the most popular side hikes of the Annapurna Circuit trek, and thousands of trekkers visit it each year to admire its spectacular landscape (Figure 1b). However, despite its touristic attractiveness, its origin has never been addressed in details. Lakes at altitudes close to the snowline generally have a glacial origin, either as proglacial lakes formed behind a frontal moraine or between a lateral moraine and the valley flank hillslope, or as lakes filling glacial cross cliff, as in the numerous Gosaikund lakes.

Tilicho Lake does not have a subaerial outlet (Figure 2). Instead, two low-elevation topographic thresholds exist: one to the west, corresponds to a pass at 5121m that leads into the Kali Gandaki watershed, and one to the east, at 4990m, that opens into the Upper Marsyandi River valley. This eastern threshold is a flat to rounded ridge 1 km wide. Even though glaciers descend from the crest of the Tilicho peaks, this rounded ridge barring the lake to the east resembles neither a lateral moraine nor a typical frontal moraine. Recently, Huber (2024) has proposed that this hill and numerous remnants of breccia deposits all around are part of a giant rockslide deposit, and that the lake formed in fact because of the upper Tilicho valley damming by this rockslide. Accordingly, this deposit would not only have blocked the Upper Marsyandi river, but would also have filled the cirque to the north, allowing the creation of other smaller lakes such as Moon Lake (Figure 2). This rockslide would have generated a rock avalanche, which would have run away along all or part of the Upper Marsyandi valley upstream from the village of Manang, i.e. more than 10 km downstream from Tilicho Lake.

Figure 1

Location map of the Tilicho rockslide.

a)

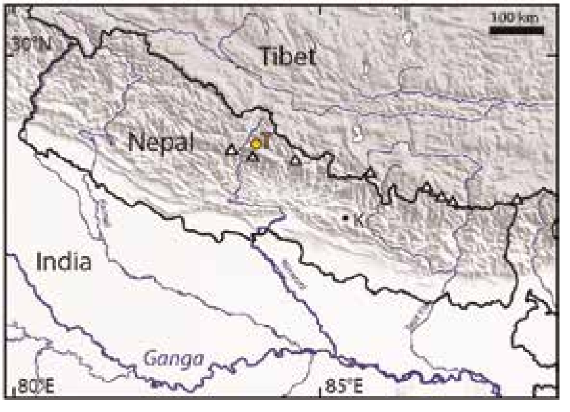

b)

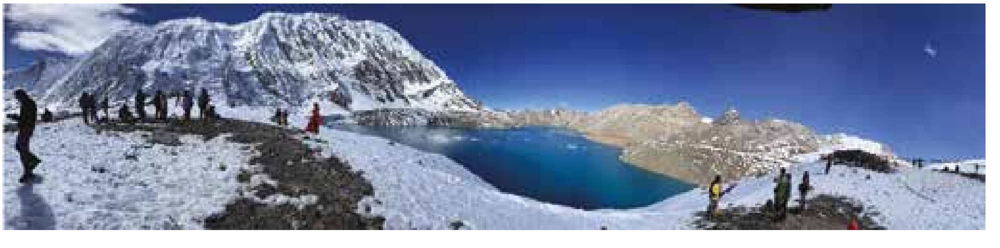

Note: (a) Map of Nepal and location of Tilicho rockslide (in yellow dot represented by 'T', K is Kathmandu). (b) Tilicho Lake with a westward view, snowy Tilicho peak rising on the left.

Figure 2

Geomorphologic map of the upper Tilicho valley and presumed Tilicho rockslide deposit taken from Huber (2024).

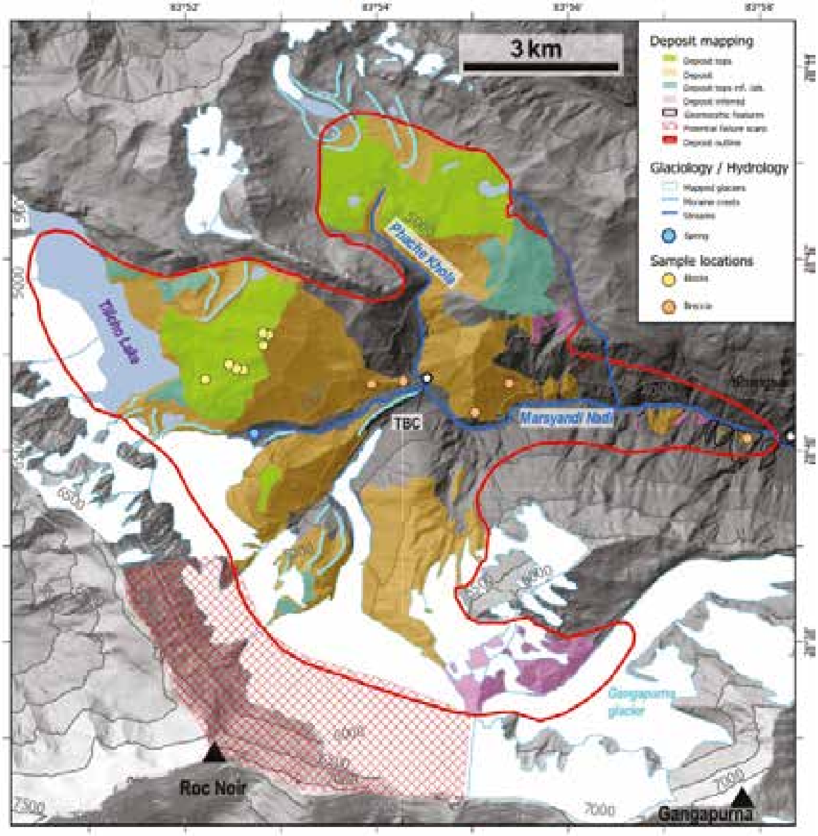

Damming of river valleys and the formation of lakes as a result of large to very large landslides is a common phenomenon in high mountainous regions (Chahal et al., 2020; Fort & Cossart, 2013; Phartiyal et al., 2009; Srivastava et al., 2013; large lake in Kirgizstan). In Nepal, the best example of such damming is Phoksundo Lake in the Dolpo region, which formed thousands of years ago when a giant rockslide that blocked the Suli Gad river ~21 kyr ago (Fort et al., 2014).

If this is the case, it has real implications in terms of natural hazard, as such giant landslide phenomena are rare but potentially extremely devastating. Understanding such hazards is crucial for risk assessment, disaster preparedness, and infrastructure development in Nepal's mountainous regions. Prevention involves identifying potentially unstable slopes and monitoring their deformation. It also involves a better understanding of the triggering factors, whether seismic or climatic, with the underlying question of the stability of Himalayan slopes in the face of current global warming.

In this paper we explore the relevance of this explanation about Tilicho Lake origin by providing new field observations, constraints on the provenance of the giant rockslide, and, after reconstructing the paleotopography of the collapsed summit, the expected geometry (extension and thickness) of the rock-avalanche deposition by a simplified numerical model compared to that documented by Huber (2024).

Geologic and Geomorphic Setting

The subduction of the Indian plate beneath the Eurasian plate created the complex geological structure of the Central Himalaya with active thrust faults, shear zones, and intense metamorphism. The Annapurna Massif, a prominent subrange of the Himalayas in north-central Nepal, is characterized by steep terrain and high-altitude conditions and is among the most geomorphologically dynamic area along the Himalayan arc. It is home to some of the world's highest peaks, including Annapurna I (8,091m), Annapurna II (7,937m), Annapurna III (7,555m), and Annapurna IV (7525m), along with numerous other prominent summits. The massif is also surrounded by deep valleys, including the Marsyandi River Valley to the east and north, and the Kali Gandaki Gorge to the west, which is one of the deepest gorges in the world.

The Annapurna Massif region is composed of a variety of rock types that pertains to some of the major Himalayan units: the High Himalayan crystallines in its southern part, and the Thetyan Sedimentary Series (TSS) in its center and northern parts, including all the high summits. These rocks have been subject to intense deformation and metamorphism over millions of years. The primary lithological units that surround the Tilicho lake include low-grade metamorphic rocks of the sedimentary sequences of the Tethyan Himalaya, made of Ordovician to Triassic impure marbles, limestone, dolomite, marl or black schists, shale and sandstones.

The Annapurna Massif experiences diverse climatic conditions, from humid subtropical zones in the southern foothills to alpine and glacial climates at higher elevations. In comparison with the southern flank of the range that received abundant precipitation during monsoon, the Tilicho area, and more largely the northern flank of the Annapurna range, displays much dryer conditions, with less than 500 mm of annual rainfall.

In the Himalayas, large-scale rockslides play a critical role in shaping the landscape, influencing river dynamics, and posing significant hazards to human settlements and infrastructure. These are one of the most significant geomorphic processes in these mountainous regions, often triggered by seismic activity, glacial retreat, permafrost degradation, and extreme weather events. Large-scale catastrophic bedrock landslide, also termed rockslide (Strom, 2019) is typically defined as a massive downslope movement of rock material, often involving the detachment and rapid displacement of rock masses over tens to hundreds of meters in vertical distance, and extending over several kilometers in horizontal distance. Among rockslides, a giant rockslide is defined as a slope failure event involving the displacement of rock masses exceeding 1 billion cubic meters. These events are characterized by the sudden mass movement of fractured rock traveling several kilometers downslope, and a high-energy impact that leads to deep fragmentation and crushing of the moving mass. They induce widespread geomorphic and ecological disturbances, both primarily disturbances resulting from the rock avalanche and potential secondary effects, including river blockages, dam formation, and outburst floods. The Annapurna massif and surrounding areas exhibit giant rockslides such as Kalopani rockslide, Braga rockslide, Latamrang rockslide, Dhukur Pokhari rockslide (Fort et al., 2009; Weidinger, 2006), and Sabche/Seti rockslide with the deposit of ~27 km^3 of highly fractured to finely crushed rock

(Lavé et al., 2023). And so recently Huber (2024) added to this long list a newly suspected giant landslide in the upper Tilicho region, an inference we test further in this study.

Field observations and Geometry of the Deposits

Field Description of the Deposit

Field investigation, were conducted mostly along the Upper Marsyandi and Phache valleys up to Tilicho and Moon lakes (Figure 2). Given the extent of the area and the technical difficulties to reach steep or exposed cliffs and hillslopes, many places were not visited but recognized on satellite images. However, since the largest and best outcrops exposing the inner part of the breccia deposit are found along the valleys, a rather exhaustive survey was proceeded.

On the way to Tilicho Base Camp (TBC), starting from the village of Khangsar, large parts of both valley flanks are covered with Quaternary formations (Figure 3). The ongoing erosion of these formations created spectacular erosion structures, which includes pinnacles, penitents and 35° steep and hillslopes devoid of vegetation but covered with long and regular talus and scree (Figure 3).

Figure 3

Pictures of the Tilicho rockslide deposit.

Note: (a) Westward view of the upper Tilicho Valley. In the foreground, there are ruins resembling erosion surfaces carved into a breccia rockslide deposit. In the background, the snowy ridge of Tilicho can be seen, with the Roc Noir positioned at the extreme left. (b) Eastward view from the trail to Tilicho Lake (in between Khangsar and TBC, within a breccia rockslide deposit) where a clear deposit extent can be observed with pinnacles and scree flowing towards Marsyandhi river. (c) Eastward view of the rockslide deposit featuring scree and pinnacles. (d) Rockslide deposit featuring the seepage discharge from Tilicho Lake on the right and glacier meltwater on the left, with Tilicho Peak visible on the far right. (e) Internal part of breccia displaying mixed matrix at the top and highly fractured rock encountered along the trail, around 300 m before TBC from Khangsar. (f) A highly weathered boulder of calc-schist sampled around the slope of Moon Lake. (g) Wide opening around the area of Moon Lake with WNW view from the Moon Lake.

The outcrops of the Quaternary formations on the way up to the TBC display facies typical of rock avalanche deposits. Along the right bank of the Marsyangdi Valley, one kilometer upstream of the village of Khansar, the breccia is made of matrix supported material with unsorted angular clasts, with a matrix finely crushed. They unconformably lie on top of glacial sediments, most likely basal till. Further upstream, 2-3 km before reaching the TBC, the outcrops display intensely fractured rock mass, alternating decametric coherent panels or blocks of fractured rock and more shattered zones where the rock mass is more fragmented and initial rock coherence has been lost. In both facies, jigsaw features are ubiquitous, and here, the breccia formation are characteristics of a typical main body facies of rock avalanche deposit with preserved large blocks and structures of the rockslide source (Hewitt et al., 2008; Weidinger et al., 2014). Such facies alternating angular, shattered rock fragments, fine matrix, jigsaw facies or large preserved fractured panels are also found just SW and West of TBC. Locally, close to TBC, the rock avalanche deposit is overlain by horizontally layered sediments, with angular clasts grading upward suggesting a deposition by debris flows and ascribed to posterior breccia reworking during the re-incision of the debris mass.

At TBC, the valley branches into the Phache Khola to the north, and opens up spectacularly towards the south, giving view to glacial chutes, morainic material in valley bottoms, and the spectacular rock faces of the Annapurna massifs that run from the Tare Kan at the East to the Tilicho Peak to the West and culminating at the Khansar Kan (or Roc Noir at 7485 masl) (Figure 2).

From the TBC, we follow a long trail that climbs steadily to a pass 900 m higher up. This pass appears as a vast undulating surface at 5000 m altitude, more than one km wide, before the path descends towards Tilicho Lake. The first part of the trail passes through a few pinnacles and breccia tours, but then winds its way through a large hillslope covered from top to bottom by slope debris and scree probably issued from Quaternary formation, since this imposing hillslope is free of any bedrock outcrops. Although the slope debris masks the exact nature of this Quaternary formation, we can get an idea by looking across the valley, on the right bank of the stream that drains toward the TBC: we can see a cliff >500 m high, with a continuous deposit of finely crushed breccia except in its upper part, where the proportion of coarse elements embedded in the matrix is greater. This huge mass of Quaternary breccia forms the dam that blocks Tilicho Lake to the SE. The upper part of the deposits and the area surrounding Tilicho Lake are relatively free of erosion, with a gently hilly topography from NE to SE, mainly reshaped locally by glaciers descending from the Tilicho ridge, Muktinath Himal and Idam Phra (Figure 2). This surface is made up entirely of debris of various sizes, with a few boulders of calcareous schists up to several meters high.

From TBC, the Phache Khola valley rises to the north. The first part of the valley is characterized by bedrock outcrops on the right bank, notably at a high cliff of Carboniferous limestone that materializes the eastern end of the Idam Phra ridge. The left bank, on the other hand, features large slopes covered with slope debris and dominated at crest level by breccia pinnacles and, further north, by bedrock. The valley end opens out onto a wide, moderately sloping hillslope formed solely of fairly fine shale limestone debris, with no bedrock outcrops. After crossing the altitude of about 5000 m, and crossing a pass almost a kilometer wide, one come to a large, undulating surface 4 km wide with depressions occupied by lakes, including Moon Lake in the eastern part of this surface. There has been virtually no erosion of this surface, and only moraines in the N and NW sections seem to have modified it. On the surface the debris are larger and somehow more elongated than those along the previous hillslope. Large to very large boulders are broadly distributed all along this surface, and they are mostly made of calcareous schist, and display deep physical weathering, along the schistosity planes (Figure 3).

To summarize, the Quaternary breccia deposits can be observed for almost 12 km between Khansar and the upstream parts of the Upper Marsyandi and Phache valleys. The debris deposition surfaces are very well preserved in the upstream parts, i.e. around Tilicho and Moon lakes. In the lower parts, downstream of the TBC, on the other hand, these breccias have been extensively eroded, leaving only veneers on the flanks of the Tilicho valley. This erosion result from the action of glaciers and mostly rivers. The facies exposed on these remnants undoubtedly indicate that the breccia origin from a massive rockslide and associated rock avalanche deposit. In addition, locally highly fragmented and finely brecciated material suggest a long runout distance of the rocky debris mass.

Rock Avalanche Extent and Volume Reconstruction of Valley Deposits

On the basis of these observations, we conclude, as Huber (2024) did, that all the facies observed correspond to rockslide and rock avalanche deposits. At this stage, however, it is difficult to ascertain the continuity of the observed facies. In particular, the Phache valley lobe has no outcrops in continuity with the breccia deposits just east of Tilicho Lake and downstream of the TBC. Even if a large colluvium slope follows in continuity on the left bank of the valley, the absence of outcrop showing the facies at the heart of the deposits makes it impossible at this stage to conclude whether all these deposits are associated with a single giant event or with two or even more rockslides events.

Despite this uncertainty, it is already possible to estimate the volumes of breccia deposited by the granular avalanche. To make such an estimate, it is first necessary to define the extent of the breccia deposits. Based on field observations and on satellite images, on which eroded breccia material can be recognized by more whitish and rugged aspect than the bedrock, Huber (2024) has proposed a wide extent for the depot. It is suspected to go up to the central Tilicho Lake to the NW, to fill the whole Phache cirque to the North locally overtopping its eastern ridge and developing in the adjacent Upper Marsyandi valley, to have reached at least the location of the Khansar village to the East, and to have covered some ridges and glacial valleys at the base of the Khansar Kan (Figure 2).

From this deposit extent, Huber (2024) also proposed a volume reconstruction, following a similar procedure as Lavé et al. (2023) for the Sabche cirque from field and satellite images observations. He first created a digital surface model (DSM) free of holes and artefact by combining ALOS World 3D 30 m resolution DSM, High Mountain Asia (HMA) 8 m resolution DSM, and a 25 m resolution DSM built from 1/50,000 digitized topographic maps of Nepal. Then the procedure followed three steps: 1. Reconstruction of the pre-failure topography of the upper Marsyandi valley by identifying the bedrock at the base of the breccia deposits and processing a triangular irregular networks (TIN) under GIS and then an interpolated grid; 2. Reconstruction of the initial rockslide deposit surface by identifying the uneroded remnants of the pristine surface of the rockslide deposit, and then interpolating in between these remnants to create a grid; 3. Subtracting the two surfaces to compute a raster map of the estimated breccia thickness just after the rockslide, and hereafter calculating the total volume of breccia.

This volume reconstruction is subject to different source of errors, mostly during the interpolation of the initial valley topography because the process assumes smooth surfaces and ignores the irregular relief that is hidden below the breccia deposit. In the case of the Tilicho rock avalanche, major erosion along the middle part of the upper Marsyandi valley prevent an accurate estimate of the initial breccia deposit, and there the surface could be seen as a minimum surface.

The initial topography (Figure 4) is a broad valley, probably carved out and inherited from the glacial advances of the Last Glacial Maximum. The post-collapse deposit surface reflects the interpolation of undulating surfaces, all of which lie between 5,000 and 5,500 m, whether in the extended cirque of the Tilicho Lake, south of it at the base of the Khansar Kan, or in the cirque of the Phache Khola. The upper surface of the rockslide debris appears as a fairly uniformly elevated surface over 50 km^2 in extent, descending progressively eastwards into the Upper Marsyandi river valley beyond the village of Khansar.

Figure 4

Volume reconstruction from Huber (2024).

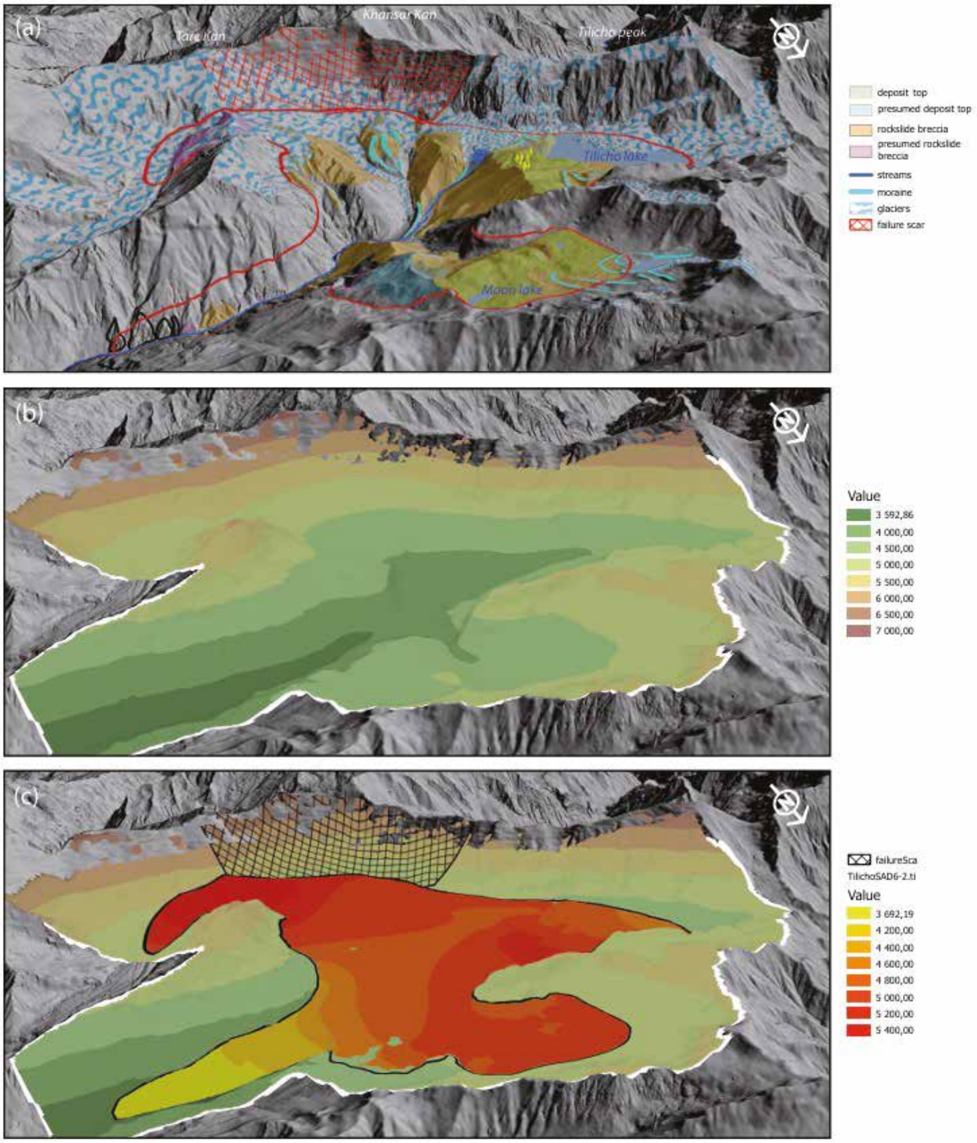

Note: (a) 3D view of the present remnants of the rock avalanche deposits; (b) estimate of the initial paleotopography before the collapse; (c) Estimate of the extent and thickness of the rock avalanche deposit just after the rockslide event.

The volume of the breccia deposit of Tilicho Rock avalanche was estimated by Huber (2024) as 21 +/- 3 km^3. On the other hand, studies show that the volume of a rockslide can increase from 7% to 26% (from the initial failed topography) when a rock mass disintegrates during the process of sliding (Hungr, 1981, p. 306; Hungr & Evans, 2004). Based on Lavé et al.'s (2023) estimate for breccia issued from TSS units, we considered the porosity of the deposit volume to be around 20%. The rock volume of the paleotopography should be around 16 ± 3 km^3. In addition, comparing initial breccia thickness and present one, Huber (2024) estimated that ~50% of the rock avalanche deposit have already been eroded to date.

Tilicho Breccia Provenance and Carbonate Isotopic Signature

Carbonate isotopic signature

Most of the rocks surrounding the Tilicho area are TSS carbonates, carbonate or marly schists with the exception of a few levels of black schists or quartzite. This makes it difficult to identify the origin of the landslide. To overcome this difficulty, we could resort to a more detailed analysis of the facies and bioclasts in thin sections, but this is a long and somehow complex procedure for finely crushed breccia matrix. An alternative is to geochemically trace these carbonates. Analysis carried out as part of Lavé et al.'s (2023) study had shown that the major stratigraphic units of the TSS had a possibly contrasting carbonate isotope signature ($\delta^{18}O$ and $\delta^{13}C$) (Figure 5 & Table 1). Based on this specificity, we analyzed new samples of bedrock to complement the existing data of Lavé et al. (2023), and especially material from the rockslide deposit, whether breccia material (clasts and matrix) or large boulders located at the top of the preserved Tilicho or Phache surfaces.

Figure 5

Geologic map of the Tilicho rock avalanche and carbonate isotopic signature.

a) b)

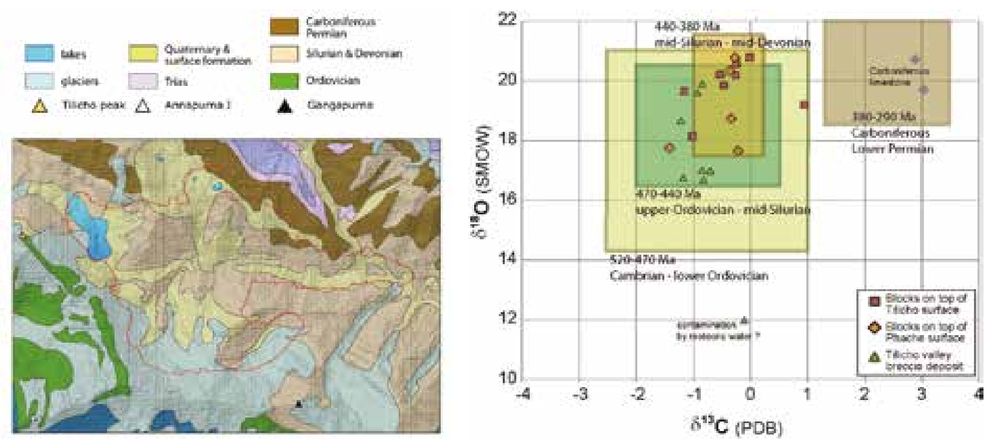

Note: (a) Geologic map of the Tilicho rock avalanche (extent delineated by the red polygon) with the main units presenting distinct isotopic signatures (map redrawn from Colchen et al., 1986). (b) (x,y) graph of the carbonate isotopic signature of the breccia and blocks sampled within and on top of the rock avalanche deposit. The rectangle delineates the range of variation of the bedrock isotopic signature of the main TSS geologic units in the region.

Table 1

Detail of Geochemical Analysis from collected samples.

Sample	Rock type	Lithology	Latitude (°N)	Longitude (°E)	Elevation (m)	$d^{18}O$ cor v-SMOW	dC^{13} corrigé PDB	$\%CaCO_3$
Rock avalanche								
UM-18-25	breccia matrix		28.6703	83.9985	3609	10.67	-0.73	75.23
UM-18-26	breccia matrix		28.6784	83.9232	4166	16.68	-0.83	50.02
UM-18-28	breccia matrix		28.6716	83.9185	4082	16.98	-0.71	48.58
UM-21-19-B	breccia matrix		28.6796	83.9237	4175	18.15	-1.02	66.88
UM-21-28	clast in breccia		28.6786	83.9046	4203	17.00	-0.85	80.35
UM-21-29	breccia material		28.6783	83.9038	4218	19.59	-0.93	68.15
UM-21-30	breccia material		28.6799	83.8998	4270	19.89	-0.85	79.91
UM-21-31	breccia material		28.6722	83.9174	4121	11.99	-0.11	49.09
UM-21-31-gA	clast in breccia		28.6722	83.9174	4121	12.64	-0.70	48.43
UM-21-31-gB	clast in breccia		28.6722	83.9174	4121	8.45	-0.33	50.09
UM-21-32	breccia matrix		28.6725	83.9174	4128	18.66	-1.22	62.57
UM-21-33	breccia material		28.6705	83.9600	3768	16.76	-1.18	49.00
UM-21-20	block on rockslide deposit	calc-schist	28.6807	83.8768	5132	20.19	-0.27	59.09
UM-21-21	block on rockslide deposit	calc-schist	28.6809	83.8756	5121	19.20	0.94	40.40
UM-21-22	block on rockslide deposit	calc-schist	28.6816	83.8743	5111	19.65	-1.17	31.47
UM-21-23	block on rockslide deposit	calc-schist	28.6790	83.8702	5020	20.22	-0.54	28.98
UM-21-24	block on rockslide deposit	calc-schist	28.6868	83.8811	5328	20.58	-0.26	70.15
UM-21-25	block on rockslide deposit	calc-schist	28.6868	83.8812	5329	20.79	-0.02	75.44
UM-21-26	block on rockslide deposit	calc-schist	28.6871	83.8802	5313	19.86	-0.47	72.81
UM-21-27	block on rockslide deposit	calc-schist	28.6849	83.8803	5294	20.25	-0.51	54.52
UM_24_18	block on rockslide deposit	calc-schist	28.7083	83.9205	5065	20.8	-0.27	91.97
UM_24_20	block on rockslide deposit	calc-schist	28.7116	83.9122	5053	20.3	-0.36	77.96
UM_24_21	block on rockslide deposit	calc-schist	28.7126	83.9120	5059	17.6	-0.21	79.29
UM_24_23	block on rockslide deposit	calc-schist	28.7042	83.9226	5069	18.7	-0.33	64.17
Bedrock								
UM_24_17	bedrock	limestone	28.6930	83.9064	4495	20.7	2.90	87.12
UM_24_24_A	bedrock	limestone	28.6947	83.9143	4734	19.7	3.04	93.11
UM_24_37	bedrock	schist	28.6888	83.9962	3971	17.7	-1.41	2.02

Carbonate content, carbon and oxygen isotopes were measured by phosphoric acid dissolution at 70°C on a gas-bench coupled to a MAT253 spectrometer. The isotopic compositions of carbonate were measured on the released CO_2 by a modified VG-602 mass spectrometer and are reported using $\delta^{18}O$ (vSMOW) and $\delta^{13}C$ (vPDB) notations. We corrected for analytical fractionation, overall uncertainty is ± 0.9% for carbonate content, and is under ± 0.2 ‰ for $\delta^{13}C$ carbon isotopic compositions (Galy & France-Lanord, 1999).

In this study, we conducted additional analyses in the substratum mainly for Permo-Carboniferous shale and Carboniferous limestone levels. While Cambrian, Ordovician, Silurian and Devonian levels show significant overlap in their range of isotopic variations, Permian and Carboniferous rocks show a highly differentiated signature with positive $\delta^{13}C$ (vPDB) values (between +1 and +4), while older lithologies all show a negative $\delta^{13}C$ signature.

The rockslide deposit samples were coming from different areas (Figure 2). The breccia clasts and matrix were sampled along the major outcrop exposing the eroded core of the rockslide deposit from upstream of Tilicho Base Camp down to the right bank of Upper Marsyandi valley south of Khangsar village. Higher in elevation at the level of the preserved surfaces of Tilicho dam or upper Phache surface, we collected mostly large blocks. All samples except one display a relatively narrow clustering for $\delta^{18}O$ (vSMOW) and $\delta^{13}C$ (vPDB) ranging between 16.5‰ and 21‰, and between -1.5‰ and 0‰ respectively.

It is important to note that there are no significant differences between the boulders collected on the Tilicho dam and upper Phache surfaces, despite the fact that the surrounding bedrock are different in terms of isotopic signature. This is consistent with a common origin of these two deposits, and in particular a non-local origin for the deposits on the upper Phache surface, since all the boulders have a negative $\delta^{13}C$ signature, incompatible with the Permo-Carboniferous terrain that structures this valley. Overall, the analyses suggest that the rockslide originated most probably in Upper Ordovician to Middle Devonian levels.

Possible Location of the Failure Surface

After analyzing the nearby topography, we found the ridges and depressions to the East, North, and West from Tilicho Base Camp too small to be able to generate a rockslide with volume larger than a few km^3. The possible collapse that could deposit such a large volume of materials must present a failure surface which would have left a huge depression or concave slope. The giant cirque-like structure at the base of Khasar Kan Peak (Figure 6a), SE from Tilicho Lake, displays a steep and around 7 km wide concave and relatively low rugosity surface over an elevation of almost 2 km. Such surface seems to fit above expected size requirements for the failure surface and appears as a good, if not the best candidate in the surrounding area, for the origin of the rockslide. In addition, according to geologic map (Colchen et al., 1986) it exposes Middle Devonian to Silurian bedrock, which is well compatible with the carbonate isotopic signature of the breccia deposits.

Although the nature of the deposits is unambiguous as to a giant rockslide origin, the geochemical elements consistent with a single event, and the source of this slide probably located on the ridge surrounding the Khansar kan, it is important to test the consistency of all the arguments, particularly with regard to the overall dynamics of the rock avalanche. In particular, we need to know whether a collapse around the Khansar kan and the rock avalanche that follows are compatible with the extension and distribution of breccia thicknesses in the Upper Marsyandi and Phache valleys (Figure 6). To carry out such a test, it is necessary to proceed in two stages. First, the volume of collapsed rock must be replaced on its original cliff face, i.e. the collapsed paleosummit must be reconstructed. Then, using a rock avalanche spread model, we can test the expected distribution of debris.

Figure 6

Khansar Kan photo (top) and Google Earth view (bottom) of the Khansar Kan ridge with the presumed surface of failure of the giant rockslide.

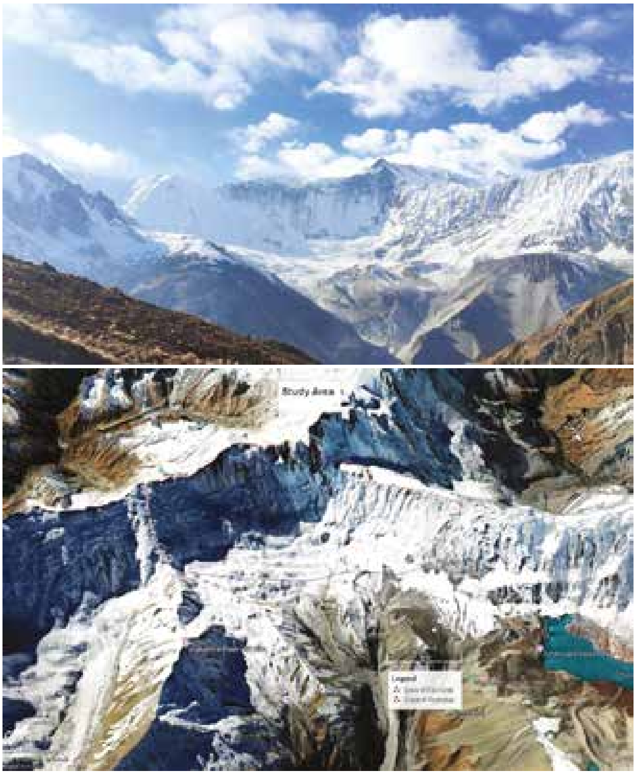

Paleo-summit Reconstruction

Method and Assumptions

To reconstruct the approximate paleo-summit, we followed the procedure proposed by (Lavé et al., 2023). For these two constraints need at least to be verified: first the restored volume of rock must equate the collapsed one, i.e. 16±3 km^3; second, the slopes and cliffs below the paleo-summit must be mechanically stable otherwise they would have failed before the giant mass through smaller rockslides.

To explore a family of possible geometries for the Khansar Kan paleo-summit, we generated topographies from fixed ground support points attached to the present ridge between Gangapurna and Tilicho Peak and from random paths for the paleo-summit crest and its northern basal footprints (Figure 6b). Whereas the elevation of the northern base footprints is interpolated from the initial cirque surface the elevation of the crest is randomly varied within a fixed range. The northern slopes between the present head scarp and the crest are allowed to vary between 40° and 50°, whereas the horizontal path respect a relative continuity of orientation with present ridge at its eastern and western terminations (Lavé et al., 2023). Intermediate points with randomly varying elevations are also generated before performing interpolation, regular grid production and volume calculation.

Different crests and baselines were initially tested in order to select a set of realistic initial topographies, i.e. family of random topographies with a majority of them matching the rock volume of the breccia deposit. Families of random topographies start from input around which random positions of basal line and ridge lines are explored in a maximum range of ~600 m and 400 m respectively (Figure 7b). To consider a paleo-topography as acceptable, besides producing a rockslide volume within 13 to 19 km^3, its hillslopes must be stable according to the criterion defined for the Annapurna region at high elevation (Lavé et al., 2023). For each randomly generated paleo-topography, a minimal safety factor is computed along all its hillslopes for potential ellipsoidal failure surfaces and considering stability from Hovland's (1977) formula. A paleo-topography is considered as acceptable in terms of hillslope stability if all the minimum factor of safety values are found to be larger than unity for an internal angle of friction of 35° in the massif and for a cohesion value C=2MPa (Lavé et al., 2023). Conversely any paleo-topography presenting factor of safety values lower than unity for these rheologic parameter values is rejected. From the final set of acceptable geometries, we calculate a mean topography, a distribution of volumes, of crest profiles and of paleo-summit elevations (Figure 7).

Figure 7

Paleo summit reconstruction.

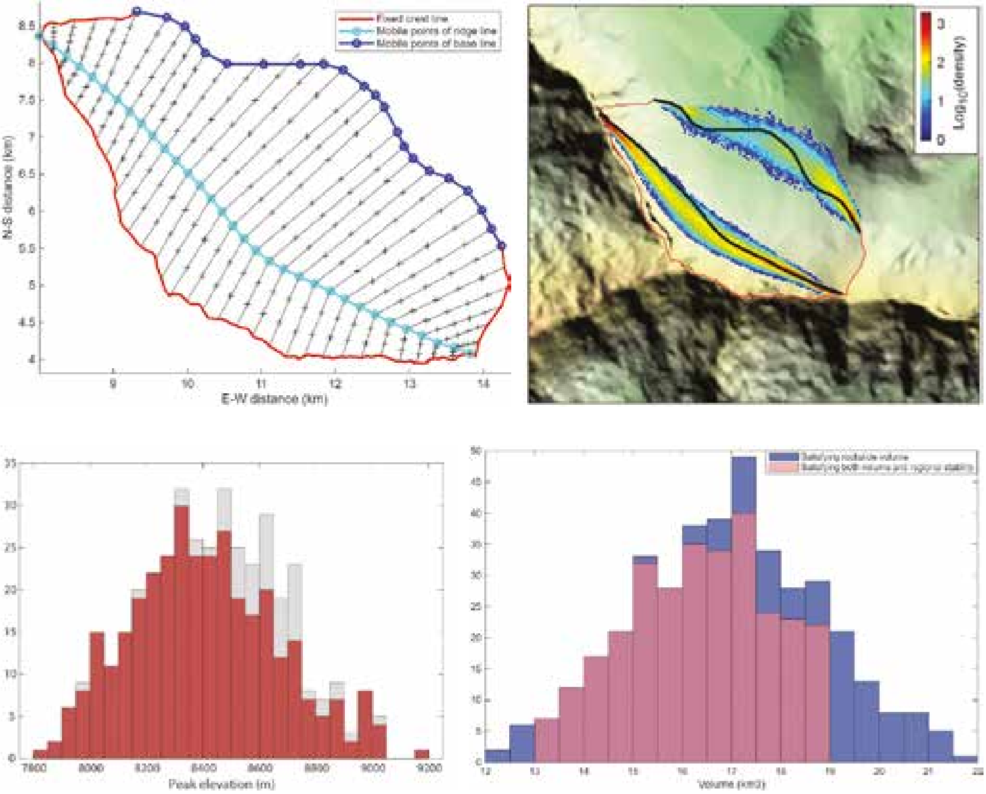

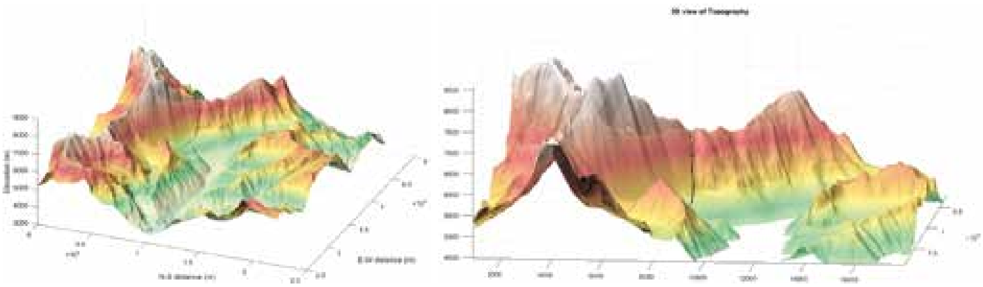

Note: (a) Constraints to build a random geometry. The red line is a fixed input crest line of the paleotopography; the blue line is one of the explored random base line of the paleotopography; cyan colored line represents one example of ridge line explored during the reconstruction of paleo-topography. Black crosses are the points that are used to construct the paleo topography of the Khangsar khan summit: their elevation are also varied randomly around the average altitude defined by uniform slope along the black lines connecting the ridge line to the base lines. (b) Density of exploration of the Ridge and Base line of the paleosummit with blue to red colors indicating increasing degree of exploration. (c) Histogram of elevation of paleo summit resulting from 400 random paleo topographies. In gray all the tested topographies, and in red the ones that fulfill the volume and hillslope stability requirements. (d) Histogram of the volume of the collapsed summit explored by the random topographies satisfying regional stability. (e) and (f) 3-D view of the mean topography of the paleosummit.

It has to be noted that the optimal ellipsoidal potential failures of the obtained paleo-topographies are shallower than the actual failure surface that led to the giant rockslide. Applying Hovland formula on this actual failure surface, and exploring various sliding directions in order to reach a minimal factor of safety, lead to a sliding direction oriented at ~25° eastward counted from the North and to a safety factor value of 1.33±0.5, well above the collapsing threshold of 1. As for the paleo-Annapurna IV (Lavé et al., 2023), we ascribe this elevated value to the fact that the rupture was probably guided by well oriented weakness planes, associated to schistosity planes or fracture families in the folded TSS large structures, which present lower values of friction angle or/and cohesion.

Results

We tested first several possible scenarios relative to the affected length of the Tilicho ridge. It turned out that to match an average volume of around 16 km^3 of rock while maintaining a reasonable base N-S width of the paleo-summit the failure zone must be more than 7 km wide, probably stretching from the Tare Kan summit along western ridge of Gangapurna to half-way between the Khansar Kan and Tilicho peaks along the Tilicho ridge.

Based on the procedure described above, we generated four hundred random possible topographies for the Khansar Kan palaeo-summit. A large majority of the rock volume range between 14.5 and 19.5 cubic kilometers. Among the 400 topographies, >80% of them were matching both volume and hillslopes stability constraints. The histogram of the maximum elevation of the acceptable geometries (red histogram) of the paleo-summit (Figure 7c) indicates that they were peaking mostly between 8000 m and 8700 m, and that the most probable peak elevation of Khansar Khan before its collapse was around 8400 m with the volume of around 17 km^3. This is 915 m above the present Khansar Kan Peak (7485 m). The paleo-summit crest was NW-SE oriented and joined the Gangapurna ridge (7455 m) at Tare Kan peak (7069 m) some 4.2 km to the east, and extended for 4 km to the north-west before joining the present-day Tilicho ridge.

Rock Avalanche Modeling

Rock Avalanche Model Description and Assumptions

In order to document the dynamics of the rock avalanche, and to test the coherence between the presumed paleosummit location and the rock avalanche deposit in terms of extent, affected area and thickness, we could rely on empirical relations between the runout distance and height drop. Such relation relates the horizontal runout distance (L), measured from the head scarp to the front of the deposit, to the height drop (H), or altitude difference between head scarp and the tip of the deposit. The ratio H/L, termed the angle of reach or fahrböschung by Heim, (1932), is found in particular to be one of the main parameters that characterize rockslide mobility (Sheidegger1973; Hsü1975; Davies 1982; Legros2002; Strom, 2019; Aaron & McDougall, 2019). However, the empirical relations need to be adapted to the valley conditions. In particular, two distinct relations are proposed (Giorio Nicoletti & Sorriso-Valvo, 1991) for unconfined or laterally confined, rock avalanches and for frontally confined valley floor. In our case, the 3D geometry of the initial valley (Figure 4) is rather complex with partial confinement at the narrow entry of the Phache valley, larger possible outlets in the western part of the Tilicho cirque and along the upper Marsyandi valley. In these conditions, the use of an empirical relation is not very adapted and do not provide distinct predictions for the various lobes of the deposit.

In our case, a numerical modeling approach seems a more appropriate approach. Numerical modeling of rock avalanches has been encompassed using many distinct codes. Whereas a few ones are 3D codes, the vast majority of theme supposed thin sheet assumption and are in fact 2D codes, in which the variables are averaged over the avalanche thickness (Savage & Hutter, 1989, 1991; Iverson, 1997; Iverson & Denlinger, 2001; Denlinger & Iverson, 2001; Heinrich et al., 2001; Patra et al., 2005). Some codes have been developed using Finite Elements approaches, a few ones using discrete elements models (Zhao et al., 2018), and many using Finite differences schemes (Bouchut et al., 2003; Kelfoun & Druin, 2005; Ouyang et al., 2013). Among these last ones, VolcFlow is a numerical modeling software developed at the Magmas and Volcanoes Laboratory (LMV) in France, that enables to simulate granular flow taking basal friction, internal friction, and volumetric spreading behavior into account (Kelfoun & Druitt, 2005). This 2D parametrization of a rock avalanche can handle shocks, rarefaction waves, and granular jumps and is stable even on complex topography. It was found to provide accurate predictions of the extent of long runout avalanches as the Socompa Rock Avalanche (Kelfoun & Druitt, 2005). VolcFlow is a finite-difference Eulerian code based on the depth-averaged approach and is developed for the simulation of isothermal geophysical flows (Kelfoun & Vargas, 2016). It uses a topography-linked coordinate system with x and y axes, parallel to the local ground surface and h perpendicular to it. The equations were solved using an original shock-capturing numerical method based on a simple or a double upwind Eulerian scheme.

Our purpose is here to test at the first order the rock avalanche trajectory, and in absence of strong constraints on the rock avalanche rheology, such a simplified 2D model appears adapted.

Volcflow model enables to vary different parameters that describe the characteristics of the granular avalanche and the boundary conditions. These parameters which are used in

Volcflow are: 1. The average density of the flow material, assumed in our case to be 2200 kg/m^3; 2. The internal friction that accounts for the frictional stress within the flow itself, between different particles or layers of the flow; 3. The cohesion, which refers to a virtual threshold stress value applied within the model to simulate certain types of flow behavior; 4. The viscosity that accounts for the flow's resistance to deformation. Higher viscosity means the flow is thicker and moves more slowly; 5. And the basal friction, which represents the friction between the moving mass and the valley bottom (Figure 8).

The density influences the flow's momentum and pressure distribution. Flows with higher density exert more force on obstacles and can travel further distances due to their greater mass. All the rheologic parameters affect the flow's ability to maintain its coherence and can influence the flow's velocity and run-out distance. In our simulations, the avalanche properties are considered as uniform and constant through time. However, to ensure that the mass has a certain coherence at the onset and behaves initially not as a fluid but as a solid undergoing essentially rotation and/or translation, before disintegrating and transforming into a fluid avalanche, an ad hoc parameter is added to the model. This parameter introduces a memory effect on material velocities that decreases exponentially with time. It corresponds to a characteristic time during which the mass remains initially coherent like a solid. An arbitrary value of 13s for this parameter proved sufficient to ensure a coherent collapse at the onset.

In terms of initial conditions, we have considered that the collapsing mass corresponds to the average topography of the "acceptable" topography (Figure 7e) and that it fails above the present geometry of the Khansar Kan Nothern face, i.e. assuming that this failure surface has been weakly modified by erosion since the rockslide. Once triggered, the avalanche is then assumed to propagate in the geometry of the Upper Marsyandi valley as defined in Figure 4

Figure 8

Evolution of the rock avalanche at 4 different times from VolcFlow.

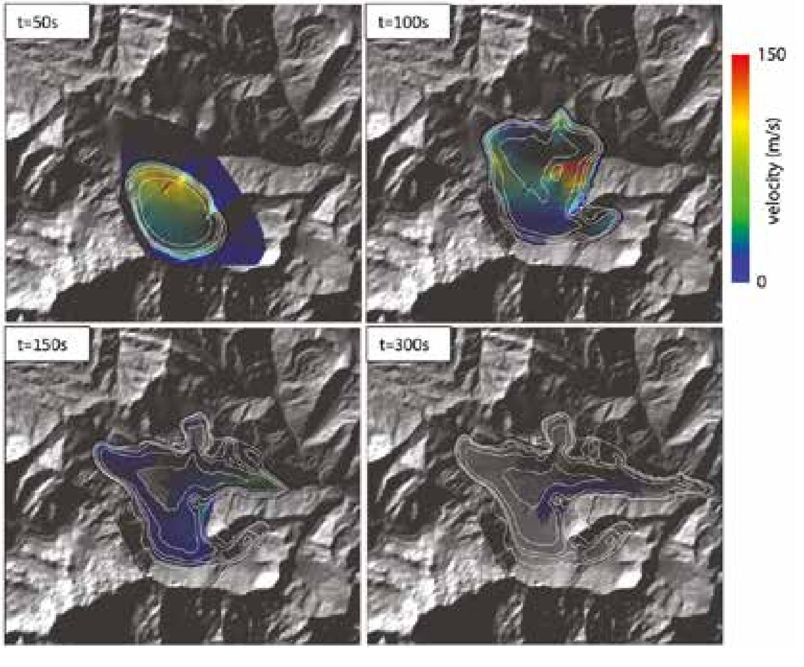

Discussion and Conclusion

We are not aware of any previous avalanche simulation with the VolcFlow code for a similar calc-schist initial lithology, and so we lack constraints on the rheological parameters of the rock avalanche mass. Therefore, we have first explored a large range of parameters values in order to find values compatible with the average extent of the rock avalanche and to define the sensitivity of the simulation results to the different parameters. This exploration indicates that a low cohesion value makes the flow behave like a fluid and spreads heavily, whereas a high cohesion value enforces the whole mass to slide down without spreading. A low value of basal friction makes the flow behave like a fluid and moves at higher speed along the valley bottom whereas a high value prevents the entire rock mass to move far away. Finally, the variation of the internal friction is comparatively of little effect on the avalanche dynamics.

The exploration tests led us to define a reference simulation characterized by the following parameters: a basal friction value of 5°, an internal friction of 12°, a rock mass cohesion of 0.2 MPa, and a rock density of 2200 kg.m^{-3}. During this simulation, the total sliding time reaches about 260 s. According to the mean velocity of the rockslide mass during the simulation (Figure 9a), the motion of the rockslide can be divided into 2 stages: first the acceleration stage when the mass rush down due to gravitational force, and secondly the deceleration phase when the mass slows down and breccia get deposited. The initial phase lasts ~80s, and the mass slides down towards NNE with minimal lateral spreading. The velocity gradually increases and peaks at 130m/s at time t=80s. At this stage, the flow hits the Idam Phra ridge that partly blocks its frontal propagation, and the lateral spreading of the flow then becomes significant. After t=87s, the velocity of flow decelerates and the rock avalanche starts to flow laterally towards E, W, and NNE directions through the different valley. The deposit quickly settles towards the west, whereas the eastern lobe still propagates along the Upper Marsyandi valley during an additional ~110s. During the second phase, even if a large fraction of the avalanche is diverted laterally by the Idam Phra ridge, a significant amount of the mass overtops this ridge or rush through the Phache valley, propagating upward in this valley and finally depositing a lobe of debris in the Phache cirque.

Figure 9

(a) Timing of the rock avalanche duration and mean velocities. (b) Comparison of the observed (Huber, 2024) extent and the modeled deposit extent. (c) The modeled breccia deposit thickness (in meter) by VolcFlow.

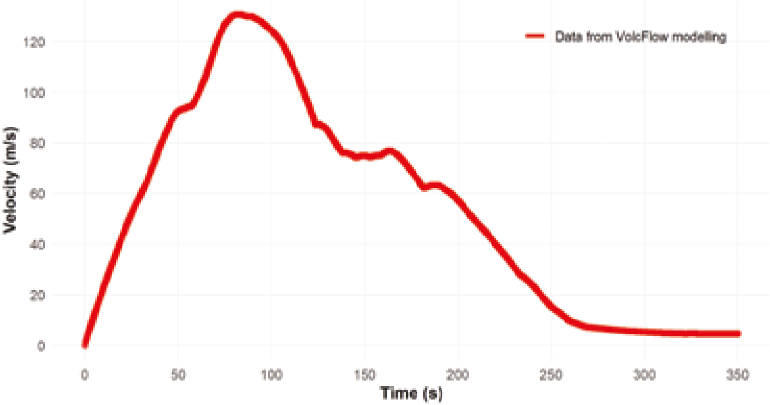

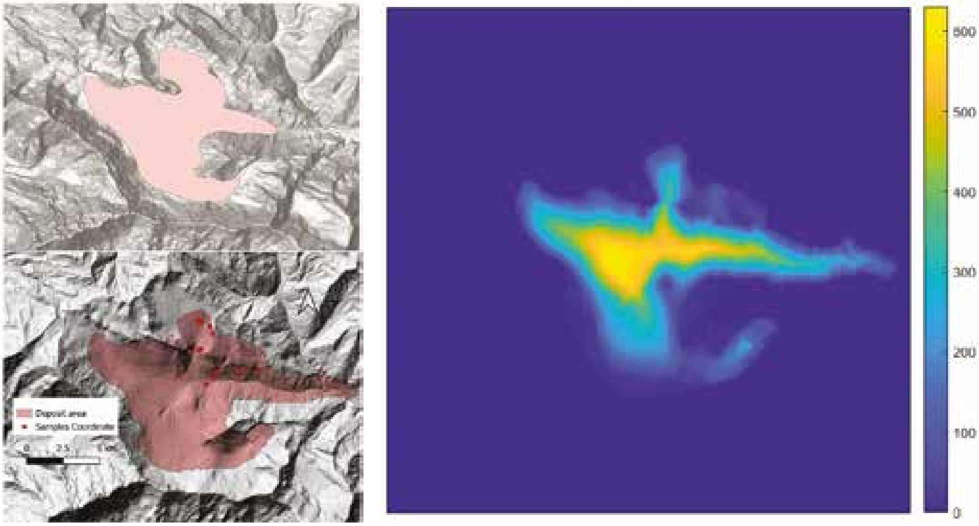

The final deposit extends over 96 km^2 (Figure 9b). Its geometry matches relatively well in most areas Huber's (2024) reconstruction of deposit extent. The main difference concerns the extent of the debris tongue toward the East in the Upper Marsyandi valley: the simulation suggests that the avalanche traveled down to Manang, whereas debris deposit ends near Khansar village in Huber's (2024) reconstruction. However, it has to be noted that this eastward extent is a minimum: the fact that the last occurrence clearly identified as belonging to the Tilicho deposit, and located on the right bank of the Upper Marsyandi river opposite Khansar, does not rule out the fact that the avalanche may have travelled further than this point.

Rather than the extension, it's more the thickness of the debris that the simulation fails to account for properly. The maximum thickness of around 620 m (Figure 9c) in the simulation represents only two third of the thickness expected below the present hill that dams the Tilicho lake or above the TBC. Instead of creating a high mound, the simulation tends to create a non-convex surface at an altitude of 4700 m (to be verified). Even if the initial valley geometry is imprecise due to the limited number of bedrock outcrop West of TBC, this modeled thickness appears significantly lower than observed. Nevertheless, if basal friction is greatly increased up to a value of 15°, a thickness > 1000 m at the deposit center can be reached, but it causes the flow to slow down and limits the extent of the Phache and westen Tilicho lobes which are much smaller than observed. In the field, we observed jigsaw facies with large fractured bedrock along the center of the deposit near TBC, suggesting whole mass sliding associated to high internal friction, whereas the material of the eastern or northern lobes seem more fragmented. Our model assumption of uniform and constant frictional parameters is an over simplification. Accounting for such variations, due for example to distinct degree of fragmentation or fluid phase (air or vapor) content, could explain both thick debris piling at the center of the avalanche and significant outer spreading due to lower apparent friction or viscosity at the margins of the avalanche. Furthermore, the presence of liquid water from melting ice and snow can play also a dominant role in basal friction and rock avalanche motion (Buss & Heim, 1881; Hungr & Evans, 2004). Spatial distribution of such water-induced friction reduction might also modulate variable mobility at the base of the rock avalanche. Future tests with a modified version of VolcFlow enabling spatial and temporal variability of the mechanical properties, as well as of the basal friction would be necessary to quantitatively test this inference. However, despite the differences in thickness, rock avalanche modeling with VolcFlow indicates that, at first order, the overall scenario proposed from observation for the origin of the Tilicho rockslide and its spreading is consistent with simulation results.

The field investigation and numerical modeling of the Tilicho rockslide provide valuable insights into the dynamics, preconditioning factors and geomorphic implications of large-scale rockslides in the Annapurna Massif. These findings not only validate previous hypotheses about large Himalayan slope failures but also extend our understanding by linking field evidence, paleo-summit reconstruction, and simulation into a coherent picture.

The deposits observed mostly around the Tilicho Base Camp display classic signatures of a high-magnitude rockslide, including jigsaw-fractured blocks, large coherent panels, and a mix of fragmented and intact boulders. These features suggest that the slide mass moved as a coherent block in some areas, while in others it fragmented during runout, likely due to internal stresses and collisions along the path. Similar deposit features were documented in other large rockslides (Lavé et al., 2023; Korup et al., 2006; Hungr & Evans, 2004). The rock avalanche deposit at Tilicho Lake (Huber, 2024) is a completely new entry in the list of rock avalanches in the central Himalayas. With an estimated deposit volume of ~21 km^3, this rock slope failure represents the second largest event to date in the central Himalayas after the rock avalanche in the Sabche cirque (volume of 27 +4/-3 km^3) (Lavé et al., 2023).

In this scenario, the giant rockslide would have blocked the upper Marsyandi and created a collosal dam that has been partially eroded in its eastern part but is still large enough to remain stable and contain the Tilicho lake's volume. This stability could be jeopardized on the long term by the incision of the debris by a stream outflowing from the lake, but the lake has the particularity of not having reached its overflow threshold. This may seem strange for a lake that is partially frozen in winter, and for which evaporation losses probably do not compensate for glacial water inflows from the south. However, this has a simple explanation. The mass of the dam is made of breccia with a high porosity (we've roughly estimated it at 20%) and therefore also has a high permeability, enabling efficient underground drainage of the lake. In fact, on the eastern flank of the dam, at an altitude of 140 m to 180 m below lake level, there are several narrow springs (Figure 3d) that combine to form a fairly powerful stream with a flow rate roughly estimated at ~3 m^3/s (the water depth averages around 30-40cm, stream width 5 to 10m, and the water velocity 1.5m/s as estimated by the floating body method)

The reconstruction of the paleo-topography revealed that the Khansar Khan paleo-summit likely stood above 8000 m, significantly higher than the current peak. This suggests that the mass involved in the rockslide was not only voluminous (~17 km^3) but also originated from extreme elevations, which explains its ability to travel long distances and even climb uphill near Moon Lake.

The VolcFlow modeling provided further information. It demonstrated that the avalanche dynamics is marked by an initial acceleration stage and subsequent lateral spreading, and that a cliff ahead on the way of the flow, can restrict the long runout and redirected good part of the flow to spread in lateral directions, even if part of the kinetic energy is also utilized to climb uphill. Such uphill overtopping associated to initial high gravitational energy is an important point to consider when building risk management and exposition maps. It also demonstrates that numerical simulation can be used at first order to document a map of exposition to natural hazard. However, the used 2D- model remains a simplified model, and its prediction needs to be considered with necessary caution: for example, simulations underestimate deposit thickness and therefore could overestimate the runout distance. In addition, the model does not predict either associated effects like dust cloud deposition, subsequent debris flows just after the collapse or during the re-incision of the mass of debris, etc. In any case, the Tilicho rock avalanche should remind us that rockslides and avalanches are among the most powerful natural processes contributing to potentially giant mass movement and reshaping of mountainous landscapes.

As far as the age and causes of this giant event are concerned - essential elements in determining the recurrence of such events in a given region, or the factors that trigger them - much remains to be done. While precise dating by cosmogenic exposure ages of boulders at the top of the deposits or by 14C dating of organic debris preserved at the base of the deposit (Lavé et al., 2023) is conceivable, the determination of the causes of a giant event is not. In the meantime, we can already say that the landslide occurred after the Last Glacial Maximum insofar as the mass of the deposits was not re-incised by the glaciers, supposed to have advanced well beyond Manang during the LGM. Determining the causes of such an event appears more complicated. Preparatory factors such as debutressing effect after the glacial retreat following the LGM, and/or a rise in permafrost that will lower the apparent cohesion of the slopes located between 4500 and 5500m can a priori be put forward. However, ascribing the trigger to for example a seismic event is risky insofar as there is no catalog of seismicity for Nepal beyond the last millennium, and the precision of the dating of both the earthquake and the landslide generally precludes a precise correlation of the respective calendars o these events.

Acknowledgment

The Paleo-summit reconstruction and stable isotopic analysis was preformed in the laboratory of the Centre de Recherches Pétrographiques et Géochimiques (CRPG), a leading Earth science institute of the French National Centre for Scientific Research (CNRS) and Université de Lorraine, located in Vandoeuvre-lès-Nancy (France), has internationally recognized expertise in geochemistry, petrology, cosmochemistry, geomorphology, and tectonics, with a strong analytical support, and has a long tradition of training and hosting international doctoral and postdoctoral researchers, supported by dedicated administrative services and integrated into European and global research networks. Special acknowledge is extended to Nepal Mountain Academy for its administrative support and facilitation of this research.

References

Aaron, J., McDougall, S. (2019). Rock avalanche mobility: The role of path material. *Engineering Geology 257* 105126

Aizaki, M., Terashima, A., Nakahara, H., Nishio, T., & Ishida, Y. (1987). Trophic status of Tilitso, a high altitude Himalayan lake. *Hydrobiologia, 153*(3), 217–224. https://doi.org/10.1007/bf00007208

Bouchut, F., Mangeney-Castelnau, A., Perthame, B., Vilotte, J.-P. (2003). A new model of Saint Venant and Savage–Hutter type for gravity driven shallow water flows. *Comptes Rendus Math. 336* (6), 531–536.

Chahal, P., Kumar, A., Sharma, P. C., Sundriyal, Y. P., & Srivastava, P. (2020). A preliminary assessment of the geological evidence of the mega floods in the upper Zanskar catchement, NW Himalaya. *Journal of the Palaeontological Society of India, 65*(1), 64-72.

Davies, T. R. (1982). Spreading of rock avalanche debris by mechanical fluidization. *Rock mechanics, 15*(1), 9-24.

Denlinger, R. P., & Iverson, R. M. (2001). Flow of variably fluidized granular masses across three-dimensional terrain: 2. Numerical predictions and experimental tests. *Journal of Geophysical Research: Solid Earth, 106*(B1), 553-566.

Fort, M., Braucher, R., Bourlès, D., Guillou, V., Rimal, L. N., Gribenski, N., & Cossart, E. (2014, April). Geomorphic impacts, age and significance of two giant landslide dams in the Nepal Himalayas: Ringmo-Phoksundo (Dolpo District) and Dhampu-Chhoya (Mustang District). In *EGU General Assembly Conference Abstracts. Vol. 16*. p. 5615).

Fort, M., & Cossart, E. (2013). Erosion assessment in the middle Kali Gandaki (Nepal): A sediment budget approach. *Journal of Nepal Geological Society, 46*, 25-40.

Fort, M., Cossart, E., Deline, P., Dzikowski, M., Nicoud, G., Ravanel, L., Schoeneich, P., & Wassmer, P. (2009). Geomorphic impacts of large and rapid mass movements: A review. *Géomorphologie : Relief, Processus, Environnement, 15*(1), 47—64-47—64. https://doi.org/10.4000/geomorphologie.7495

Galy, A., & France-Lanord, C. (1999). Weathering processes in the Ganges–Brahmaputra basin and the riverine alkalinity budget. *Chemical Geology.* http://www.sciencedirect.com/science/article/pii/S0009254199000339

Hewitt, K., Clague, J. J., & Orwin, J. F. (2008). Legacies of catastrophic rock slope failures in mountain landscapes. *Earth-Science Reviews, 87*(1–2), 1–38. https://doi.org/10.1016/j.earscirev.2007.10.002

Hovland, H. (1977). Three-dimensional slope stability analysis method. *J. Geotech. Engrg. Div., 103*(9), 971-986. https://doi.org/10.1061/ajgeb6.0000493

Hsu, K. J. (1975). Catastrophic debris streams (sturzstroms) generated by rockfalls. *Geological Society of America Bulletin, 86*(1), 129-140.

Huber, M., (2024), Dynamics of large bedrock landslides, numerical modelling and Himalayan case studies, PhD thesis manuscript, Université de Lorraine

Hungr, O. (1981). Dynamics of rock avalanches and other types of slope movements, PhD Thesis, Edmonton University.

Hungr, O., & Evans, S. G. (2004). Entrainment of debris in rock avalanches: An analysis of a long run-out mechanism. *Geological Society of America Bulletin, 116*(9), 1240. https://doi.org/10.1130/B25362.1

Iverson, R. M. (1997). The physics of debris flows. *Reviews of geophysics, 35*(3), 245-296.

Iverson, R. M., & Denlinger, R. P. (2001). Flow of variably fluidized granular masses across three-dimensional terrain: 1. Coulomb mixture theory. *Journal of Geophysical Research: Solid Earth, 106*(B1), 537-552.

Kelfoun, K., & Druitt, T. H. (2005). Numerical modeling of the emplacement of Socompa rock avalanche, Chile. *Journal of Geophysical Research: Solid Earth, 110*(B12), 2005JB003758. https://doi.org/10.1029/2005JB003758\

Kelfoun, K., & Vargas, S. V. (2016). VolcFlow capabilities and potential development for the simulation of lava flows. *Geological Society, London, Special Publications, 426*(1), 337–343. https://doi.

org/10.1144/SP426.8

Korup, O., Strom, A. L., & Weidinger, J. T. (2006). Fluvial response to large rock-slope failures: Examples from the Himalayas, the Tien Shan, and the Southern Alps in New Zealand. *Geomorphology, 78*(1–2), 3–21. https://doi.org/10.1016/j.geomorph.2006.01.020

Lavé, J., Guérin, C., Valla, P. G., Guillou, V., Rigaudier, T., Benedetti, L., France-Lanord, C., Gajurel, A. P., Morin, G., Dumoulin, J. P., Moreau, C., & Galy, V. (2023). Medieval demise of a Himalayan giant summit induced by mega-landslide. *Nature, 619*(7968), 94–101. https://doi.org/10.1038/s41586-023-06040-5

Legros, F. (2002). The mobility of long-runout landslides. *Engineering Geology, 63*(3–4), 301–331. https://doi.org/10.1016/S0013-7952(01)00090-4

Losen, J., Rizza, M., Nutz, A., Henriquet, M., Schuster, M., Rakhmedinov, E., ... & Siame, L. (2024). Repeated failures of the giant Beshkiol Landslide and their impact on the long-term Naryn Basin floodings, Kyrgyz Tien Shan. *Geomorphology, 453*, 109121."

Nicoletti, P. G., & Sorriso-Valvo, M. (1991). Geomorphic controls of the shape and mobility of rock avalanches. *Geological Society of America Bulletin, 103*(10), 1365–1373. https://doi.org/10.1130/0016-7606(1991)103%3C1365:GCOTSA%3E2.3.CO;2

Ouyang C., SimingHe, A. B. N., QiangXu, C., YuLuo A. B., Wencheng Zhang, A., MacCormack, TVD. (2013). Finite difference method to simulate the mass flow in mountainous terrain with variable computational domain. *Computers & Geosciences 52* 1–10

Phartiyal, B., Sharma, A., Srivastava, P., & Ray, Y. (2009). Chronology of relict lake deposits in the Spiti River, NW Trans Himalaya: Implications to Late Pleistocene–Holocene climate-tectonic perturbations. *Geomorphology, 108*(3-4), 264-272.

Savage, S. B., & Hutter, K. (1989). The motion of a finite mass of granular material down a rough incline. *Journal of fluid mechanics, 199*, 177-215.

Savage, S. B., & Hutter, K. (1991). The dynamics of avalanches of granular materials from initiation to runout. Part I: Analysis. *Acta Mechanica, 86*(1), 201-223.

Scheidegger, A. E. (1973). On the prediction of the reach and velocity of catastrophic landslides. *Rock Mechanics and Rock Engineering, 5*(4), 231-236.

Srivastava, P., Ray, Y., Phartiyal, B., & Sharma, A. (2013). Late pleistocene-holocene morphosedimentary architecture, Spiti River, arid higher Himalaya. *International Journal of Earth Sciences, 102*(7), 1967-1984.

Strom, A. (2019). Large-Scale Rockslide Inventory of the Central Asia Region: Data and Analysis. In A. Shakoor & K. Cato (Eds.), IAEG/AEG Annual Meeting Proceedings, San Francisco, California, 2018—Volume 1 (pp. 145–153). Springer International Publishing. https://doi.org/10.1007/978-3-319-93124-1_18

Weidinger, J. T. (2006). Predesign, failure and displacement mechanisms of large rockslides in the Annapurna Himalayas, Nepal. *Engineering Geology, 83*(1–3), 201–216. https://doi.org/10.1016/j.enggeo.2005.06.032

Weidinger, J. T., Korup, O., Munack, H., Altenberger, U., Dunning, S. A., Tippelt, G., & Lottermoser, W. (2014). Giant rockslides from the inside. *Earth and Planetary Science Letters, 389*, 62–73. https://doi.org/10.1016/j.epsl.2013.12.017

Zhao, T., Crosta, G. B., Dattola, G., & Utili, S. (2018). Dynamic fragmentation of jointed rock blocks during rockslideavalanches: Insights from discrete element analyses. *Journal of Geophysical Research: Solid Earth, 123*, 3250–3269. https://doi.org/10.1002/2017JB015210